

# Response of circular footing on dry dense sand to impact load with different embedment depths

Adnan F. Ali<sup>1a</sup>, Mohammed Y. Fattah<sup>\*2</sup> and Balqees A. Ahmed<sup>1b</sup>

<sup>1</sup>Civil Engineering Department, University of Baghdad, Baghdad, Iraq

<sup>2</sup>Building and Construction Engineering Department, University of Technology, Baghdad, Iraq

(Received July 13, 2017, Revised February 22, 2018, Accepted February 24, 2018)

**Abstract.** Machine foundations with impact loads are common powerful sources of industrial vibrations. These foundations are generally transferring vertical dynamic loads to the soil and generate ground vibrations which may harmfully affect the surrounding structures or buildings. Dynamic effects range from severe trouble of working conditions for some sensitive instruments or devices to visible structural damage. This work includes an experimental study on the behavior of dry dense sand under the action of a single impulsive load. The objective of this research is to predict the dry sand response under impact loads. Emphasis will be made on attenuation of waves induced by impact loads through the soil. The research also includes studying the effect of footing embedment, and footing area on the soil behavior and its dynamic response. Different falling masses from different heights were conducted using the falling weight deflectometer (FWD) to provide the single pulse energy. The responses of different soils were evaluated at different locations (vertically below the impact plate and horizontally away from it). These responses include; displacements, velocities, and accelerations that are developed due to the impact acting at top and different depths within the soil using the falling weight deflectometer (FWD) and accelerometers (ARH-500A Waterproof, and Low capacity Acceleration Transducer) that are embedded in the soil in addition to soil pressure gauges. It was concluded that increasing the footing embedment depth results in increase in the amplitude of the force-time history by about 10-30% due to increase in the degree of confinement. This is accompanied by a decrease in the displacement response of the soil by about 40-50% due to increase in the overburden pressure when the embedment depth increased which leads to increasing the stiffness of sandy soil. There is also increase in the natural frequency of the soil-foundation system by about 20-45%. For surface foundation, the foundation is free to oscillate in vertical, horizontal and rocking modes. But, when embedding a footing, the surrounding soil restricts oscillation due to confinement which leads to increasing the natural frequency. Moreover, the soil density increases with depth because of compaction, which makes the soil behave as a solid medium. Increasing the footing embedment depth results in an increase in the damping ratio by about 50-150% due to the increase of soil density as D/B increases, hence the soil tends to behave as a solid medium which activates both viscous and strain damping.

**Keywords:** circular footing; dry sand; embedment depth; displacement; impact

## 1. Introduction

Dynamic response of soil subjected to dynamic loads will be governed by the dynamic soil properties. The responses obtained for different dynamic loadings needs to be back analyzed to determine the dynamic soil properties (Kumar *et al.* 2013). The properties that are most important for dynamic analyses are the stiffness, damping ratio, and unit weight. These enter directly into the computations of dynamic response. In addition, the location of the water table, degree of saturation, and grain size distribution may be important, especially when liquefaction is a potential problem.

Stress wave propagation is of extreme importance in geotechnical engineering, since it allows determination of soil properties such as modulus of elasticity, shear wave

velocity, shear modulus; interpretation of test results of geophysical investigation, numerical formulation of ground response analysis and also helps in the development of the design parameters for earthquake resistant structures (Das and Ramana 2011).

Elastic waves that travel from sources of dynamic and produce elastic soil deformations (ground vibrations) vary in magnitude depending on the intensity of the propagated waves. The responses of structures to ground vibrations depend on the soil-structure interaction. However, under certain circumstances such as a combination of cohesionless soil layers and ground vibrations, elastic waves can be the reason for plastic soil deformations, e.g., liquefaction, densification and soil settlements. The structural response to ground excitation depends on the soil response to waves propagated from the source and soil-structure interaction (Svinkin 2008).

Al-Homoud and Al-Maaitah (1996) found that for forced vibration tests, there is an increase in natural frequency and a reduction in amplitude with the increase in embedment depth. On the other hand for free vibration test, the results showed that for different footing models resting

\*Corresponding author, Professor  
E-mail: myf\_1968@yahoo.com

<sup>a</sup>Professor

<sup>b</sup>Assistant Lecturer

on sandy soil, there is an increase in damping ratio with increasing the depth of embedment.

Mandal and Roychowdhury (2008) presented the central response of the square raft under the step loading of 100 kN for different depth to width ratios. It was observed that the increase in the depth of embedment yields response of lesser amplitude and higher frequency.

Xue *et al.* (2012) investigated experimentally and numerically the damage fatigue problem of a hammer foundation system with fatigue damage growth and the influences of damage and vibration on the machine foundation. The responses of ground soil near the foundation block due to the impact of hammer blows were discussed using the concept of damage mechanics based on the interaction between hammer foundation damage and soil ground damage. From analysis of the simulated results, conclusions could be obtained that when a machine foundation is subjected to strong dynamic loading, the dynamic response increases significantly with the degree of damage. This in turn influences the damage propagation both in the foundation and the soil due to the higher stresses concentrating near the foundation areas. Furthermore, the natural frequencies of the hammer foundation system are reduced significantly with the damage growth and as the damping ratio increases significantly. From the numerical investigation of the dynamic properties of damage in the soil ground, it could be seen that the influences of hammer blows on both surface and depth of the soil near the foundation are significant when damage increases. This provides the possibility to work out a method for controlling the damage and its growth in a damaged material, as well as the dynamic response of a damaged structure.

Bhandari and Sengupta (2014) when investigating the foundation embedment concluded that with increase in depth of embedment, there is decrease in value of total vibration response of foundation in vertical direction. This indicates that foundation should be embedded as deep as possible to take benefit of adjoining confining soil to carry energy waves to reduce the total vibration response. But initially at depth equal to 0.5 m, 1.0 m and 1.5 m, sudden increase in amplitude of vertical vibration was observed. It is mainly because vertical vibration is due to combined effect of vertical and rocking response. If natural frequency of the foundation in rocking response is considered, it was observed that at depths of 0.5 m, 1.0 m and 1.5 m, the natural frequency of the foundation is very close to operating frequency of machine. This creates possibility of resonance which causes increase in amplitude. This condition is arising because of embedment of foundation. For surface foundation, the foundation is free to oscillate in vertical, horizontal and rocking mode. But after introduction of embedment, the surrounding soil restricts free oscillation in rocking mode due to confinement. This has caused decrease in natural frequency for rocking vibration and it becomes nearly equal to operating frequency of machine. This is going to cause resonance in foundation vibration which will affect life of foundation. Hence, either foundation should be embedded deep in soil or its base area should be increased to avoid value of

frequency ratio becoming equal to 1.

A three dimensional soil-structure interaction (SSI) was numerically simulated by Jayalekshmi *et al.* (2014) using finite element method in order to analyze the foundation moments in annular raft of tall slender chimney structures incorporating the effect of openings in the structure and the effect of soil flexibility, when the structure-soil system is subjected to 1940 El Centro ground motion in time domain. The transient dynamic analysis is carried out using LS-DYNA software. The linear ground response analysis program ProShake has been adopted for obtaining the ground level excitation for different soil conditions, given the rock level excitation. The radial and tangential bending moments of annular raft foundation obtained from this SSI analysis have been compared with those obtained from conventional method according to the Indian standard code of practice, IS 11089:1984. It is observed that tangential and radial moments increase with the increase in flexibility of soil. The analysis results show that the natural frequency of chimney decreases with increase in supporting soil flexibility. Structural responses increase when the openings in the structure are also considered.

A dynamic numerical analysis of strip machine foundation was carried out by Fattah *et al.* (2015). The foundation of multiple thicknesses was placed at different depths above a saturated sand with different states (i.e., loose, medium and dense), and vertical harmonic excitation was applied with buildup of the excess pore water pressure being considered. The dynamic analysis was performed numerically using finite element software, PLAXIS 2D. The soil was assumed as an elastic perfectly plastic material obeying Mohr-Coulomb yield criterion. A parametric study was carried out to evaluate the dependency of machine foundation on various parameters including the amplitude of the dynamic load, the frequency of the dynamic load and the embedment of foundation. It was concluded that increasing the embedment ratio causes a reduction in the dynamic response up to a certain embedment depth; when the depth of embedment increases higher than 1 m, the effect become less pronounced. As strength of the soil increases, the effect of embedment depth in reducing the dynamic response will decrease also. The vertical displacements decrease obviously by 46, 37 and 40 % for loose, medium and dense sand, respectively, when increasing the embedment of foundation from 0.5 to 1 m, while when the embedment of foundation increases from 1 to 1.5 m, the vertical displacements for loose, medium and dense sand decrease by 45, 38 and 3 %, respectively. Finally, when the embedment of foundation increases from 1.5 to 2 m, the decrements in vertical displacements are also recorded for loose, medium and dense sand by 42, 36 and 18 %, respectively.

Guellil *et al.* (2017) when investigating the soil and structural uncertainties on impedance functions and structural response of a soil-shallow foundation-structure (SSFS) system using Monte Carlo simulations, showed that the uncertainties on shear wave velocity and thickness of the soil layer, the height of the structure and the foundation radius significantly affect the impedance functions, and in same time the response of the coupled system. Firstly, two

distribution functions (lognormal and gamma) were used to generate random numbers of soil parameters (layer's thickness and shear wave velocity) for both horizontal and rocking modes of vibration with coefficients of variation ranging between 5 and 20%, for each distribution and each parameter. Secondly, the influence of uncertainties of soil parameters (layer's thickness, and shear wave velocity), as well as structural parameters (height of the superstructure, and radius of the foundation) on the response of the coupled system using lognormal distribution was investigated. This study illustrated that uncertainties on soil and structure properties, especially shear wave velocity and thickness of the layer, height of the structure and the foundation radius significantly affect the impedance functions, and in same time the response of the coupled system.

The response and behavior of machine foundations resting on dry and saturated sand was investigated experimentally by Fattah *et al.* (2017). In order to investigate the response of soil and footing to steady state dynamic loading, a physical model was manufactured. The manufactured physical model could be used to simulate steady state harmonic load at different operating frequencies. Total of (84) physical models were performed. The parameters that were taken into considerations include loading frequency, size of footing and different soil conditions. The footing parameters were related to the size of the rectangular footing and depth of embedment. Two sizes of rectangular steel model footing were used (100×200×12.5 mm) and (200×400×5.0 mm). The footing was tested in all parameters at the surface and at 50 mm depth below model surface. Meanwhile the investigated parameters of the soil condition included dry and saturated sand for two relative densities 30% and 80%. The response of the soil to dynamic loading includes measuring the stresses inside the soil using piezoelectric sensors as well as measuring the excess pore water pressure by using pore water pressure transducers. It was found that the rate of increase in excess pore water pressure ratio decreased remarkably at a depth of 0.5 B-1.5 B (B is the footing width) for medium and loose dense sand, respectively. Moreover, excess pore water pressure ratio increases with increasing the eccentricity of dynamic load. The generated pore water pressure is always greater under the point of load application. Its value reduces with a certain percentages at any point away from the point of load application.

The objective of this research is to predict the dry sand response under impact loads. Emphasis will be made on attenuation of waves induced by impact loads through the soil. The work also includes studying the effect of footing embedment, and footing area on the soil behavior and its dynamic response.

## 2. Experimental work

Physical modeling of interesting geotechnical problems has helped in clarifying behaviors and failure mechanisms of many civil engineering systems. Physical modeling in a laboratory may be used to test the mechanics associated with a range of natural problems that have direct to

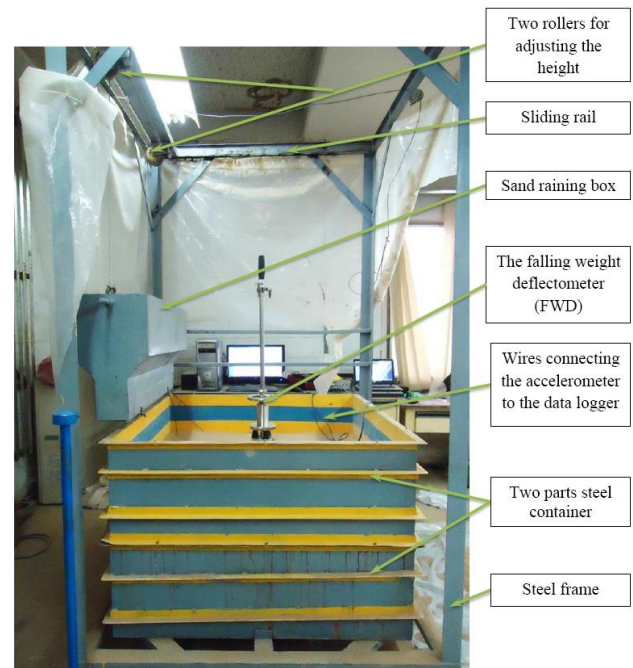


Fig. 1 The setup of the soil model

geotechnical participation together with the mechanisms that set these problems. Close control over material properties and well defined boundary conditions in physical models make declaration parametric studies to be managed (Davies *et al.* 2010).

The dynamic system is the soil medium through which waves propagate outward from sources of impact load. The input signal of the system is the impulse response of the ground at the place of installation of a machine foundation; the output signal is the dynamic response of a location of interest situated on a foundation receiving impulse or within the soil stratum.

The testing program consists of 32 tests. The tests were performed in dense soil state only under impact load with different energy forces. Two footing sizes were adopted and the models were tested at the surface of the soil and at depths of 0, 0.5B, B, and 2B (where B is the diameter of the footing).

In this study, systematic experiments are performed to investigate the dynamic response of foundation on a soil medium under the effect of impact load. Fig. 1 shows the setup that was used to carry out tests. It consists of a steel box with walls made of plates 2 mm thick and a base as a soil container, and the falling weight deflectometer (FWD) to apply impact loads on the soil model with a base bearing plate of two sizes which is dealt with as a shallow foundation on the soil under impact load. The steel box consists of two parts with dimensions; length of 1200 mm, width of 1200 mm and height of 800 mm. Each part has a height of 400 mm and strengthened from the outside with loops of 40 mm right angle 2 mm thick spaced at 1330 mm in the tangential direction.

The soil used for the model tests is clean sand, passing through sieve No. 10 and retaining on sieve No. 100. It was brought from Kerbelaa (Al-Ekhetther region) west of

Table 1 Physical properties of the used sand

Property	Value	Unit	Standard of the test
Specific Gravity, $G_s$	2.65	----	ASTM D 854 [5]
Coefficient of gradation, $C_c$	0.79	----	ASTM D 422 [8]
Coefficient of uniformity, $C_u$	2.94	----	
USCS-soil type	SP	----	
Maximum dry unit weight, $\gamma_{dmax}$	17.8	kN/m <sup>3</sup>	ASTM D 2049-69 [6]
Minimum dry unit weight, $\gamma_{dmin}$	14.9	kN/m <sup>3</sup>	ASTM D4254-00 [7]
Maximum void ratio ( $e_{max}$ )	0.7447	----	-----
Minimum void ratio ( $e_{min}$ )	0.4605	----	-----

Table 2 Physical properties of the remolded sand used in the tests

Property	Value	Unit
Dense state relative density, $D_r$ , %	82.0	----
Dry unit weight in dense state	17.2	kN/m <sup>3</sup>
Saturated unit weight in dense state	20.52	kN/m <sup>3</sup>
Void ratio at dense state	0.5114	----

Baghdad in Iraq. Physical properties of the sand are presented in Table 1.

The “raining technique and tamping” were used to deposit the soil in the testing tank at a known and a uniform density. The sand raining device consists of a steel hopper, with dimensions of 1200 mm in length, 300 mm in width and 450 mm in height, it is ended with an inclined funnel mounted above the testing tank and used as a hopper to pour the testing material from different heights through two rollers. In order to facilitate the horizontal movement of the steel tank, a simple sliding system was prepared for this purpose.

Tamping and raining technique were used to prepare the sand in the test tank. Table 2 shows the physical properties of the soil used in the tests. In order to achieve a uniform layer with a desired density, the raining technique was used to prepare the sandy soil model as shown in Fig. 2(a). This process was implemented using a pre-manufactured steel hopper and steel tank (manufactured by Al-Saffar 2015) through a repeated horizontal movement of the hopper which was controlled manually on the steel tank. The height of drop and the rate of discharge of the sand mainly affect the density of the sand layer in the raining method (Turner and Kulhawy 1987). Two rollers fixed at the top of the box were used to adjust the height of the raining device to control the height of the free fall of the sand. Several trials with different heights of fall were performed in order to achieve the desired relative density. In each trial, samples collected in small metal tins of known volumes positioned at several places in the test tank were used to check the density. After calculating the density, the void ratios of the sand and the relative density ( $D_r$ ) as a function of the height of fall, the results are presented in graphs.

To prepare the dense state of sand with relative density



(a)



(b)

Fig. 2 Preparation of sand layer (a) Sand raining technique (b) Preparation of dense sand using tamping

of 80%, the height of the free fall will be 600 mm. After filling the raining box (tank) with sand and choosing the proper height of drop 600 mm, the sand was poured into the test tank. The soil layer was prepared in 6 layers with 100 mm constant height for each one to attain the last elevation of 600 mm from the bottom of container. Then tamping is made with a hammer of 15 kg weight four times at the surface of each layer as shown in Figure 2b, the thickness of each layer was 50 mm to prepare dense sand at a relative density of 80%.

### 2.1 Measurement devices

The vertical impact load tests are conducted to simulate different impact loads using different falling masses (5 kg or 10 kg) with different dropping heights (500 mm or 250 mm). Two sizes of the base bearing plate were used; 100 mm and 150 mm.

The response of the soil under impact load was measured by installing four accelerometers; two in the vertical direction at depths equal to B and 2B where B is the diameter of the base bearing plate that was used in the test. Other two accelerometers were used in the horizontal direction at determined distances from the source of the impact load at B and 2B from the plate center and buried at a depth of 10 mm from the surface. The system of acquisition data was utilized so that all data could be scanned and recorded automatically.

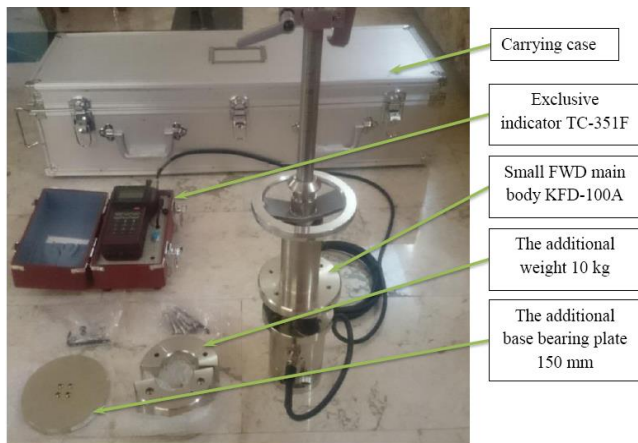


Fig. 3 The small FWD system with the standard set with accessories that were used in tests

To examine the boundary effect for testing setup, a single test was performed for the case of the highest impact load and it was found that there is no reasonable dynamic response at the boundary of the model.

In this research, the falling weight deflectometer (FWD) was used to apply impact loads on the soil model. The small FWD system with the standard set with options Measurement/ Analysis Software TC-7100, additional weight (10 kg), and loading plate of 150 mm diameter were used as shown in Fig. 3. This equipment is capable of measuring the applied impact force-time history, displacement-time history at the soil surface, the modulus of elasticity of the soil, and the coefficient of subgrade reaction.

During each test, the acceleration-time history was measured at different depths utilizing accelerometers transducers (ARH-A waterproof, low capacity acceleration transducer (ARH-500A)) type. The basic structure of the FWD system consists of the main unit with built-in accelerometer (KFD-100A) as shown in Fig. 3 and the indicator (TC-351F). The indicator records the maximum load value, maximum displacement value and the analyzed coefficient of subgrade reaction and subgrade modulus. Various analysis results can be recorded and stored in the memory card. The data recorded in the memory card can be taken into a PC directly or via the indicator. The indicator system is capable of getting the reading every 0.05 msec. In addition, in this research, the load, acceleration, velocity, displacement waveform, O-P time (in case of load: time between the start point of loading and the maximum value point, in case of displacement: time between the start point of loading of displacement and the maximum value point of displacement), and time product are stored in the PC in addition to the analysis results from the indicator because the measurement/processing software (TC-7100) was used.

This system drops the weight of the small FWD main body by free fall and measures the impact load and displacement using the load cell and the accelerometer. Displacement is measured by integrating the measurement value in the accelerometer twice. The measurement/processing software (TC-7100) is required for a measurement system that uses a PC. In this system, the data



(a)



(b)



(c)

Fig. 4 Devices for dynamic response measurement (a) The used transducers, (b) The accelerometer with its catalogue, (c) The transducer connection to data logger

transferred to the indicator is transferred to the PC as it is via the indicator.

Fig. 4 shows four accelerometers (ARH-500A Waterproof, Low capacity Acceleration Transducer) to measure acceleration in the sand. They are connected to the multi-recorder TMR-200 to analyze the data measured by the transducers.

ARH-A waterproof, low capacity acceleration transducer (ARH-500A) was used. It is installed in water or ground or embedded in concrete. The rigid waterproof structure makes this transducer suitable for use in an adverse environment or for outdoor use.

The details of abbreviation for the tested samples as well as example of models naming are explained in Table 3.

## 2.2 Testing procedure

The following steps describe the testing methodology:

1. Preparing the layers of sand which have a total depth of 400 mm (100 mm for each) as mentioned before depending on the required relative density.

2. Installing the accelerometers at the center of the sand

Table 3 Details of the testing program and test designation

No.	Test designation	Soil state	Soil density	Impact loading state	Size of bearing plate (mm)	The dropping mass (kg)	The height of drop (mm)
1	DD <sub>s</sub> P <sub>10</sub> M <sub>5</sub> H <sub>50</sub>	Dry	Dense	at surface	100	5	500
2	DD <sub>0.5b</sub> P <sub>10</sub> M <sub>5</sub> H <sub>50</sub>	Dry	Dense	at 0.5 B	100	5	500
3	DD <sub>b</sub> P <sub>10</sub> M <sub>5</sub> H <sub>50</sub>	Dry	Dense	at B	100	5	500
4	DD <sub>2b</sub> P <sub>10</sub> M <sub>5</sub> H <sub>50</sub>	Dry	Dense	at 2B	100	5	500
5	DD <sub>s</sub> P <sub>15</sub> M <sub>5</sub> H <sub>50</sub>	Dry	Dense	at surface	150	5	500
6	DD <sub>0.5b</sub> P <sub>15</sub> M <sub>5</sub> H <sub>50</sub>	Dry	Dense	at 0.5 B	150	5	500
7	DD <sub>b</sub> P <sub>15</sub> M <sub>5</sub> H <sub>50</sub>	Dry	Dense	at B	150	5	500
8	DD <sub>2b</sub> P <sub>15</sub> M <sub>5</sub> H <sub>50</sub>	Dry	Dense	at 2B	150	5	500
9	DD <sub>s</sub> P <sub>10</sub> M <sub>10</sub> H <sub>50</sub>	Dry	Dense	at surface	100	10	500
10	DD <sub>0.5b</sub> P <sub>10</sub> M <sub>10</sub> H <sub>50</sub>	Dry	Dense	at 0.5 B	100	10	500
11	DD <sub>b</sub> P <sub>10</sub> M <sub>10</sub> H <sub>50</sub>	Dry	Dense	at B	100	10	500
12	DD <sub>2b</sub> P <sub>10</sub> M <sub>10</sub> H <sub>50</sub>	Dry	Dense	at 2B	100	10	500
13	DD <sub>s</sub> P <sub>15</sub> M <sub>10</sub> H <sub>50</sub>	Dry	Dense	at surface	150	10	500
14	DD <sub>0.5b</sub> P <sub>15</sub> M <sub>10</sub> H <sub>50</sub>	Dry	Dense	at 0.5 B	150	10	500
15	DD <sub>b</sub> P <sub>15</sub> M <sub>10</sub> H <sub>50</sub>	Dry	Dense	at B	150	10	500
16	DD <sub>2b</sub> P <sub>15</sub> M <sub>10</sub> H <sub>50</sub>	Dry	Dense	at 2B	150	10	500
17	DD <sub>s</sub> P <sub>10</sub> M <sub>5</sub> H <sub>25</sub>	Dry	Dense	at surface	100	5	250
18	DD <sub>0.5b</sub> P <sub>10</sub> M <sub>5</sub> H <sub>25</sub>	Dry	Dense	at 0.5 B	100	5	250
19	DD <sub>b</sub> P <sub>10</sub> M <sub>5</sub> H <sub>25</sub>	Dry	Dense	at B	100	5	250
20	DD <sub>2b</sub> P <sub>10</sub> M <sub>5</sub> H <sub>25</sub>	Dry	Dense	at 2B	100	5	250
21	DD <sub>s</sub> P <sub>15</sub> M <sub>5</sub> H <sub>25</sub>	Dry	Dense	at surface	150	5	250
22	DD <sub>0.5b</sub> P <sub>15</sub> M <sub>5</sub> H <sub>25</sub>	Dry	Dense	at 0.5 B	150	5	250
23	DD <sub>b</sub> P <sub>15</sub> M <sub>5</sub> H <sub>25</sub>	Dry	Dense	at B	150	5	250
24	DD <sub>2b</sub> P <sub>15</sub> M <sub>5</sub> H <sub>25</sub>	Dry	Dense	at 2B	150	5	250
25	DD <sub>s</sub> P <sub>10</sub> M <sub>10</sub> H <sub>25</sub>	Dry	Dense	at surface	100	10	250
26	DD <sub>0.5b</sub> P <sub>10</sub> M <sub>10</sub> H <sub>25</sub>	Dry	Dense	at 0.5 B	100	10	250
27	DD <sub>b</sub> P <sub>10</sub> M <sub>10</sub> H <sub>25</sub>	Dry	Dense	at B	100	10	250
28	DD <sub>2b</sub> P <sub>10</sub> M <sub>10</sub> H <sub>25</sub>	Dry	Dense	at 2B	100	10	250
29	DD <sub>s</sub> P <sub>15</sub> M <sub>10</sub> H <sub>25</sub>	Dry	Dense	at surface	150	10	250
30	DD <sub>0.5b</sub> P <sub>15</sub> M <sub>10</sub> H <sub>25</sub>	Dry	Dense	at 0.5 B	150	10	250
31	DD <sub>b</sub> P <sub>15</sub> M <sub>10</sub> H <sub>25</sub>	Dry	Dense	at B	150	10	250
32	DD <sub>2b</sub> P <sub>15</sub> M <sub>10</sub> H <sub>25</sub>	Dry	Dense	at 2B	150	10	250

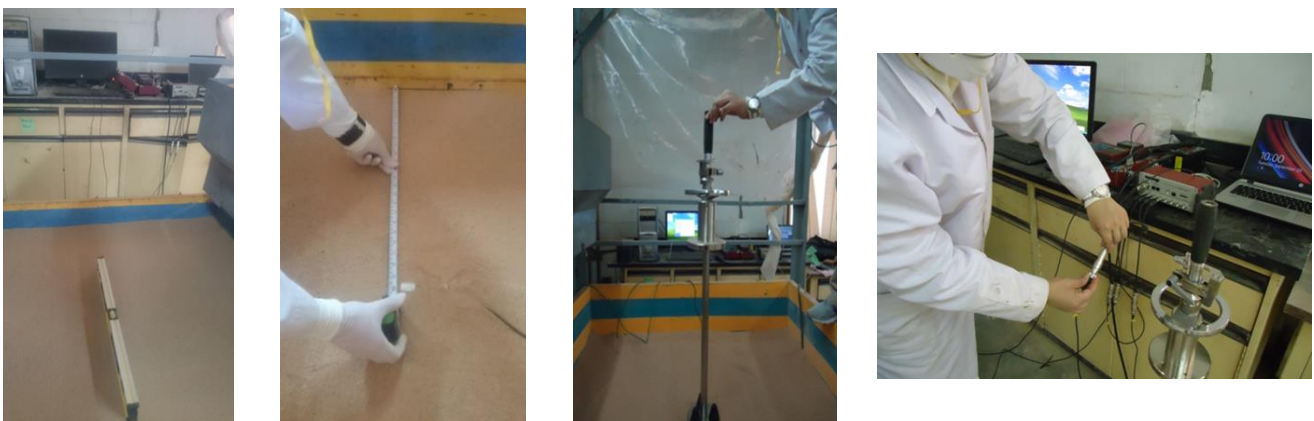


Fig. 5 Steps of preparing the physical model

layer in the vertical direction under the centroid of the bearing plate at a depth of (B) or (2B) according to the size of bearing plate.

3. Installing the accelerometer in the horizontal direction near the surface at a depth of 10 mm.

4. Leveling the surface and installing the FWD at the center of the model surface and checking if it is perpendicular to the surface of the model.

5. Adjusting the data logger reader and the exclusive indicator TC-351F of the FWD to get zero readings.

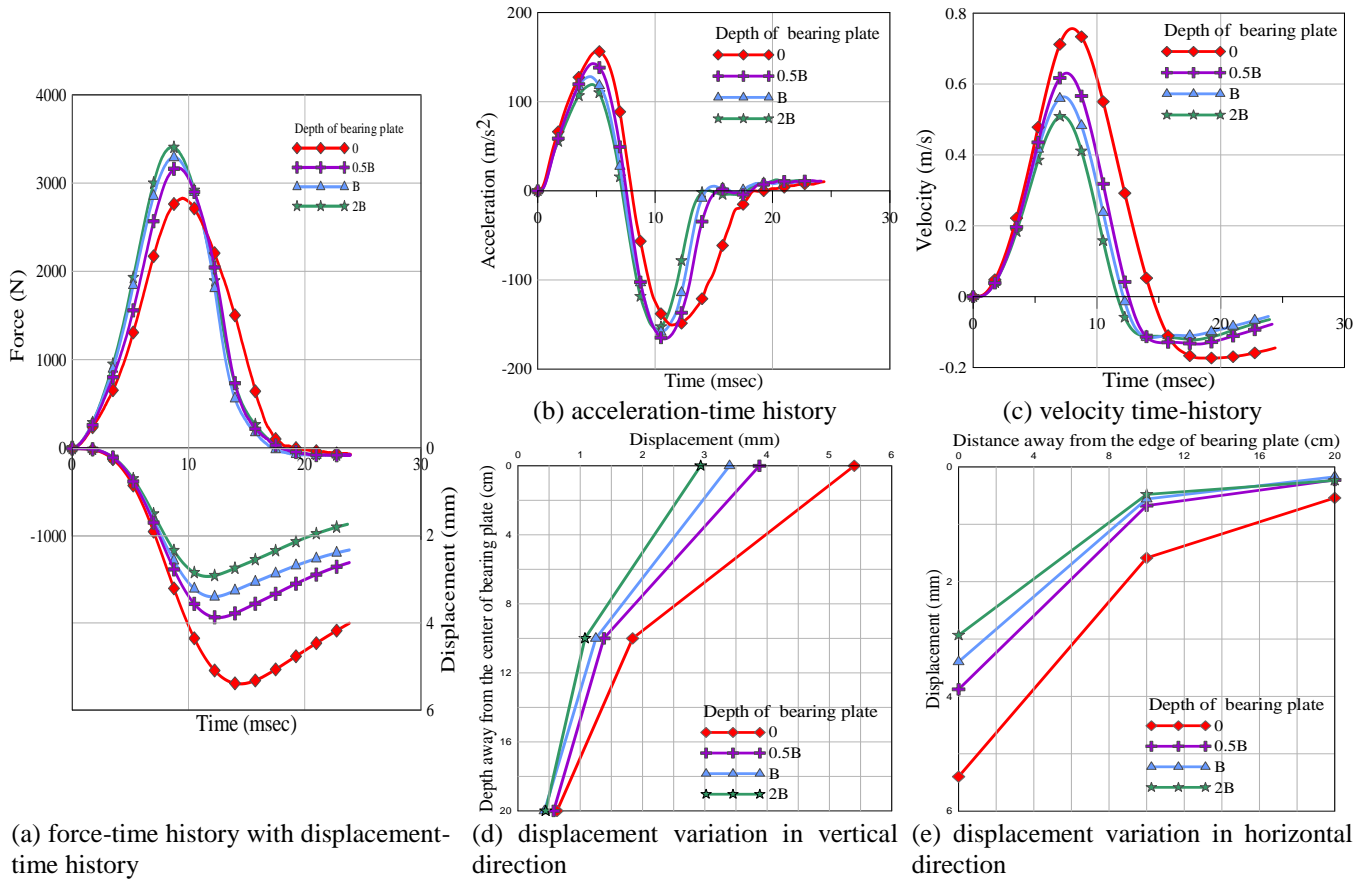


Fig. 6 Test results for  $DDP_{10}M_5H_{50}$  model

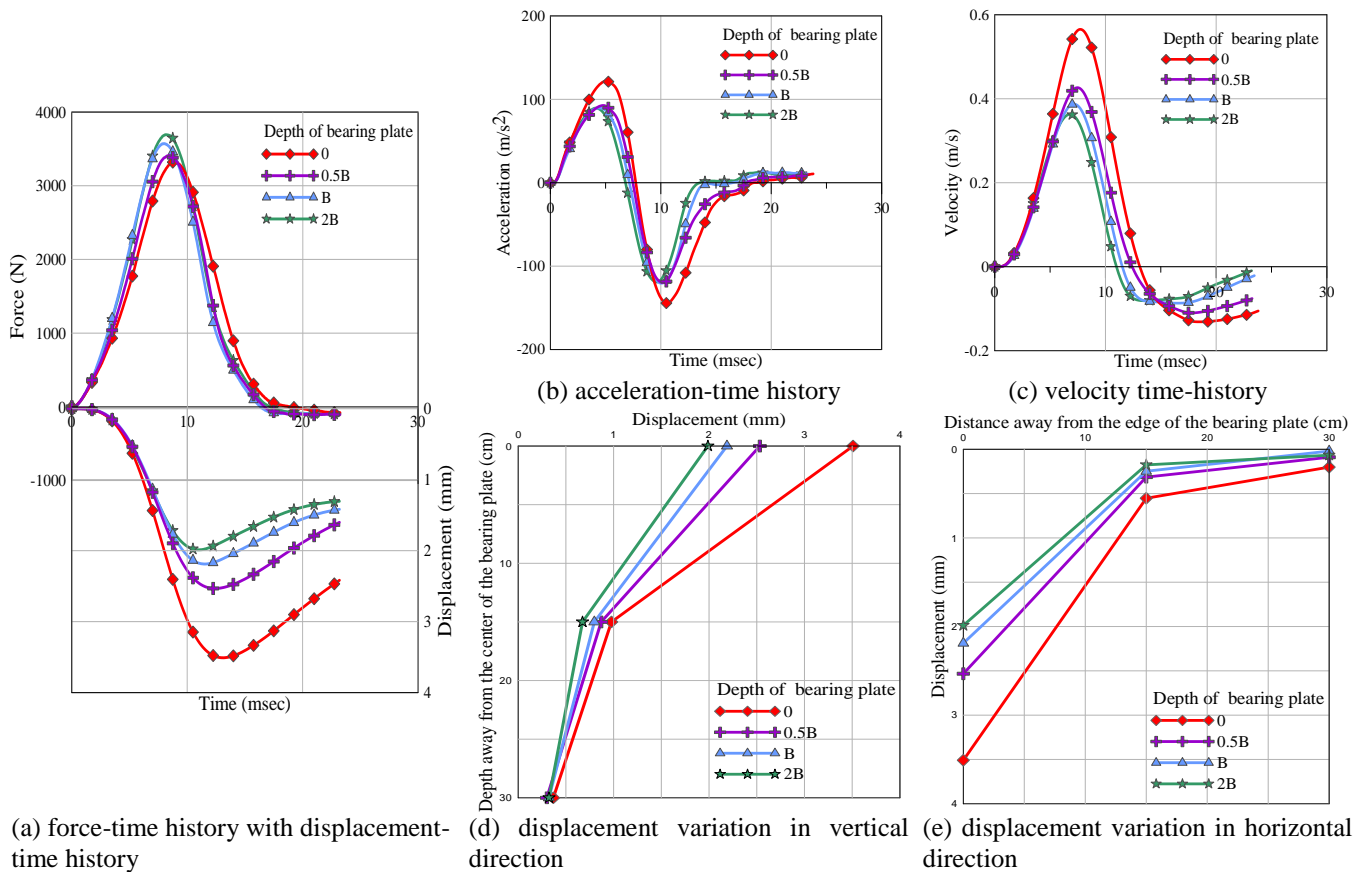


Fig. 7 Test results for  $DDP_{15}M_5H_{50}$  model

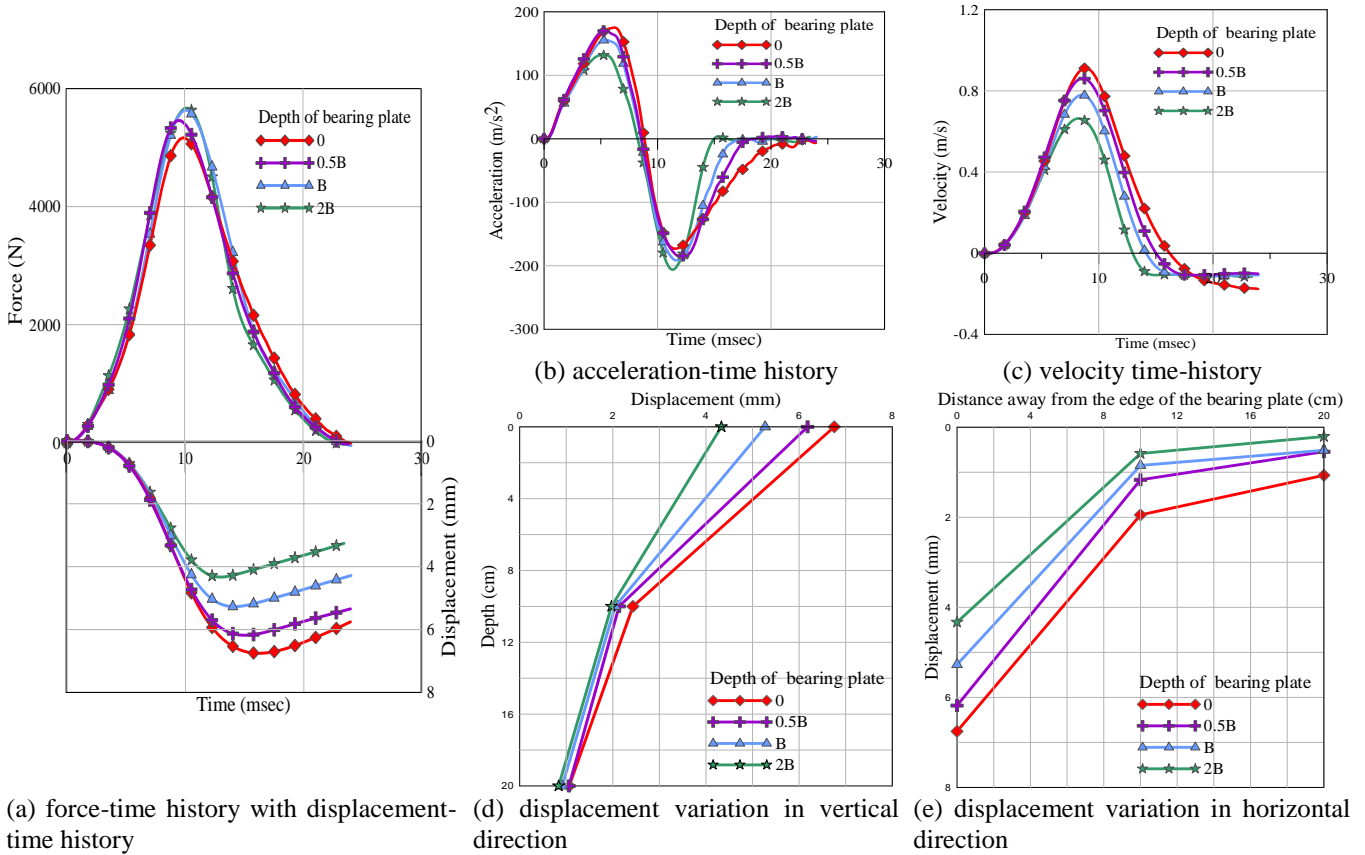


Fig. 8 Test results for  $DDP_{10}M_{10}H_{50}$  model

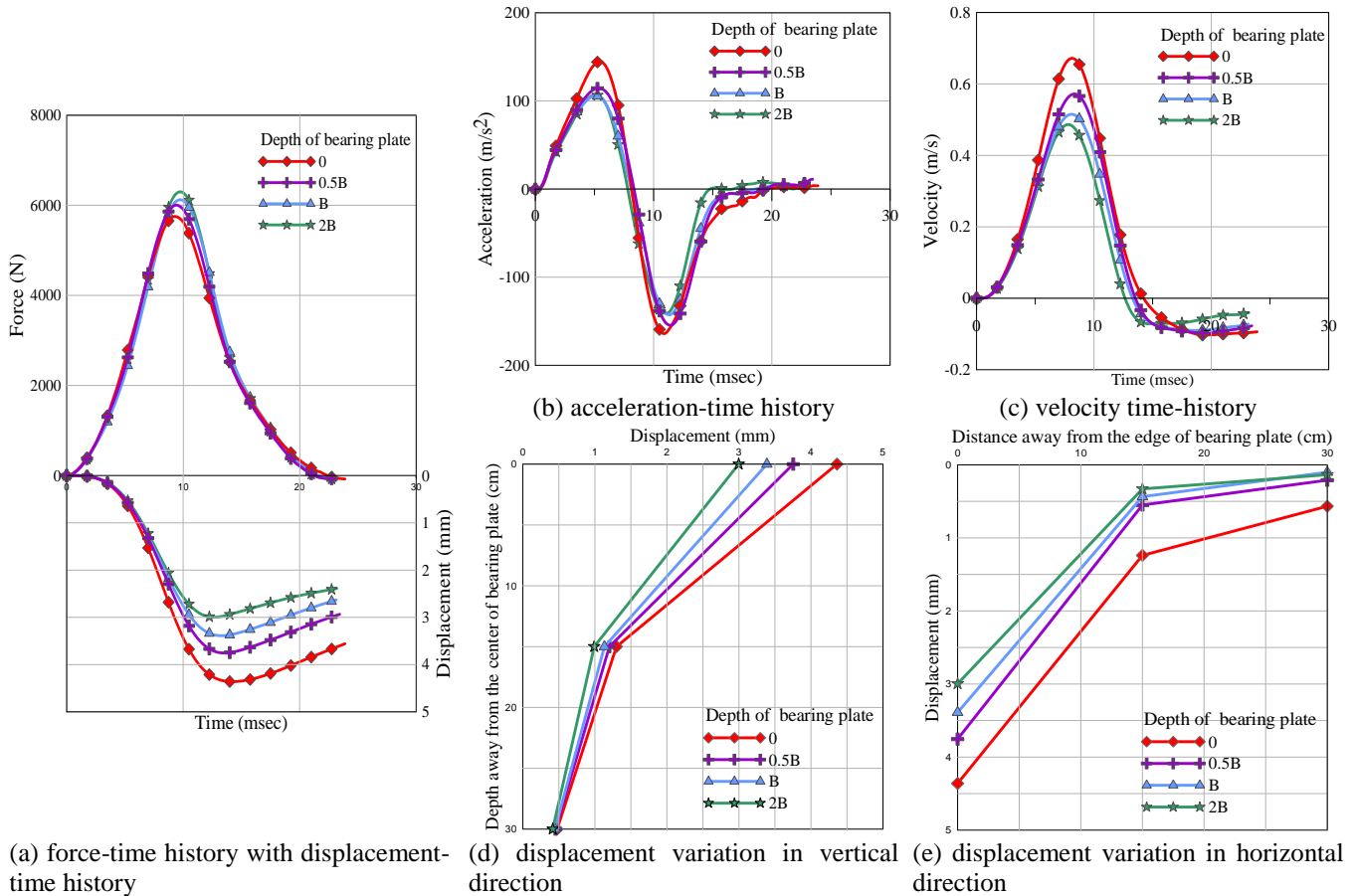
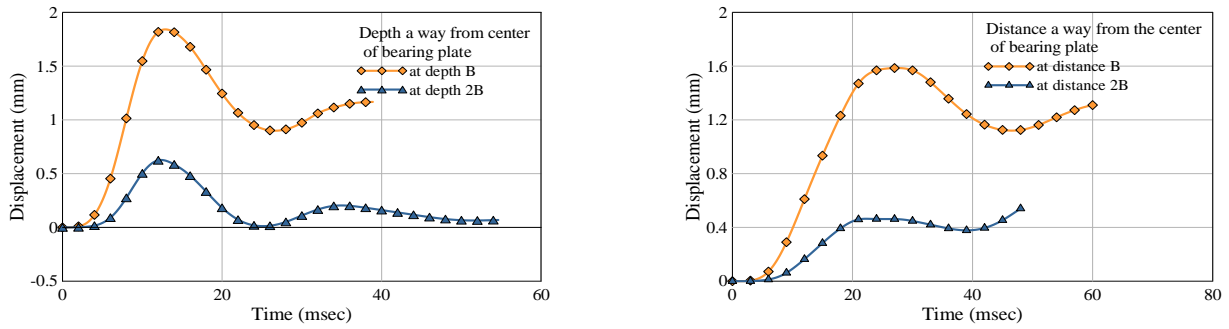
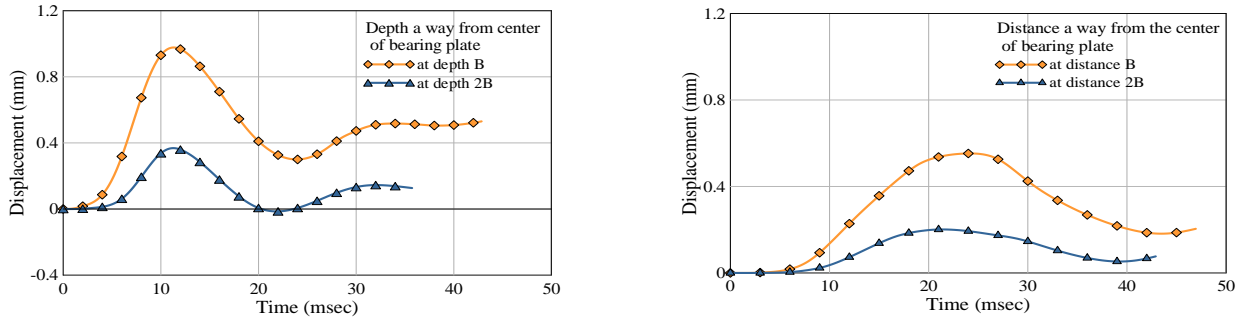


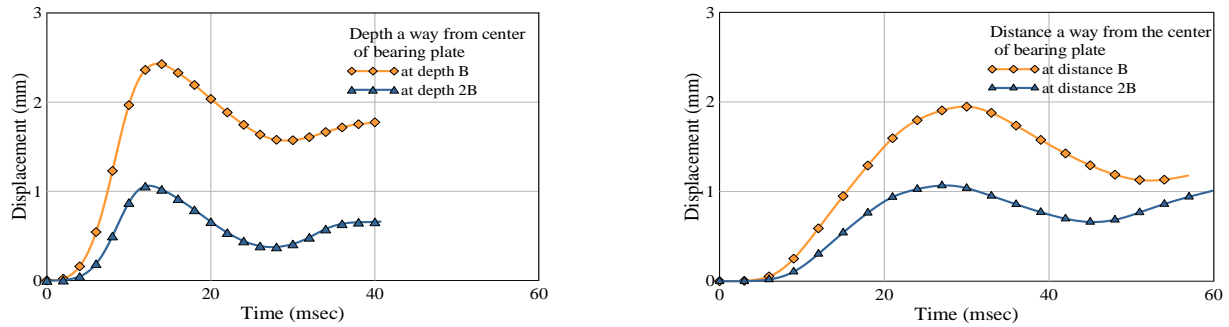
Fig. 9 Test results for  $DDP_{15}M_{10}H_{50}$  model



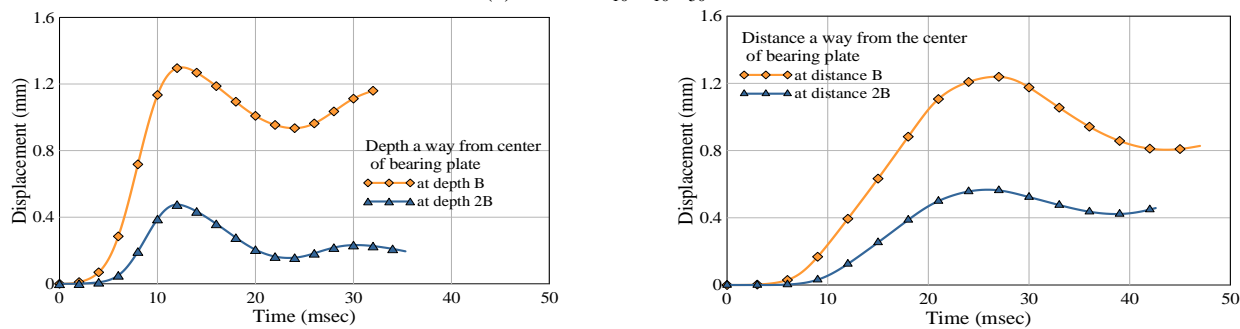
(a) for  $DDP_{10}M_5H_{50}$  model



(b) for  $DDP_{15}M_5H_{50}$  model



(c) for  $DDP_{10}M_{10}H_{50}$  model



(d) for  $DDP_{15}M_{10}H_{50}$  model

Fig. 10 Displacement response when the bearing plate at surface

6. Releasing the striking mass and the resulted response will be recorded and presented on a PC.

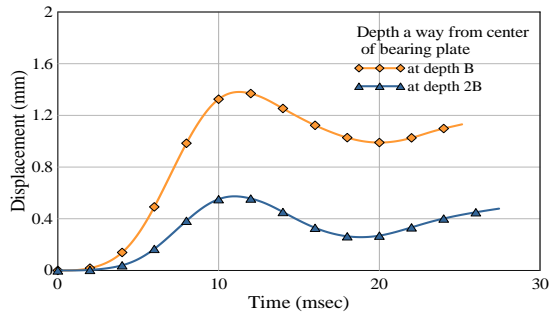
Fig. 5 shows some steps of preparing the physical model.

### 3. Results and discussion

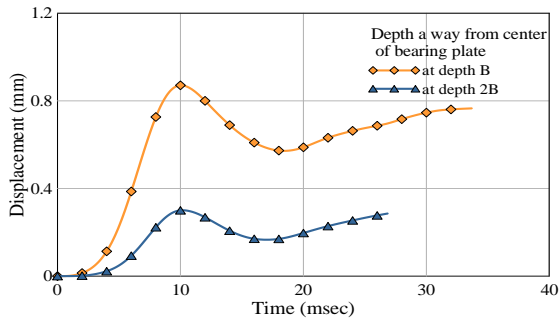
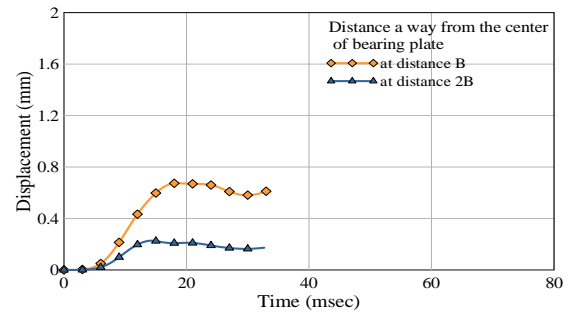
Impact tests were carried out on dense dry sandy soils with different loading parameters. Two bearing plate sizes, 100 mm or 150 mm were used, the plate was placed at the

soil surface or at depths of  $0.5B$ ,  $B$ , or  $2B$ . The impact load was applied by dropping a mass of 5 kg or 10 kg from a height of 500 mm or 250 mm. Test results are presented in Figs. 6 to 9. These results include the load-time history, displacement, acceleration, and velocity functions of time as shown in parts (a, b, and c) of each figure for each response, respectively. All these responses are measured under the plate directly.

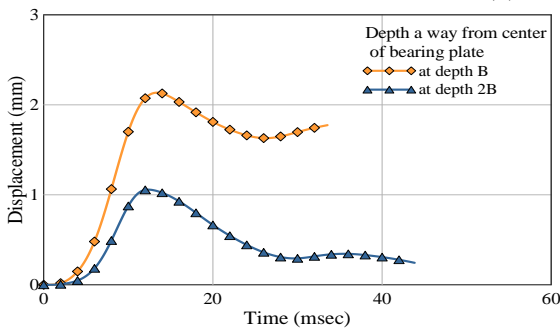
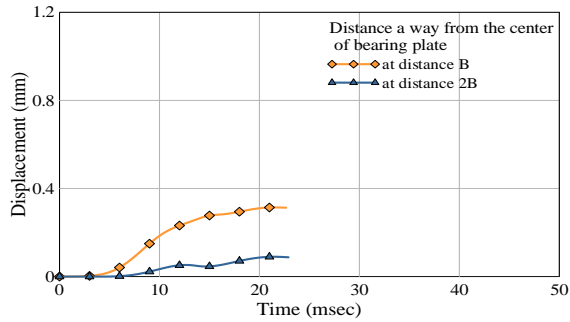
Parts (d and e) of each figure show the variation of vertical displacement (beneath the plate) and horizontal displacement (at a distance from the edge of the plate) with



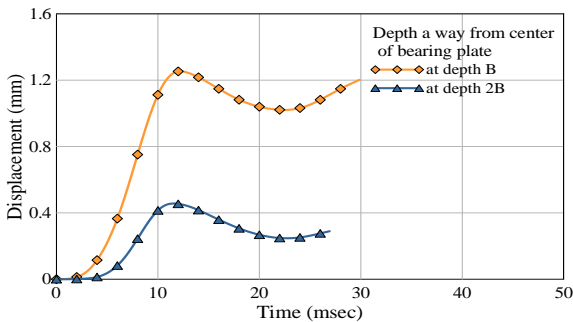
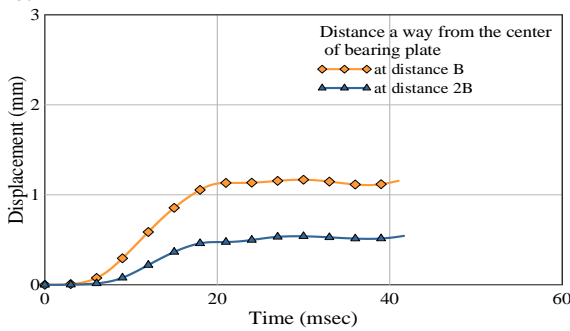
(a) for DDP<sub>10</sub>M<sub>5</sub>H<sub>50</sub> model



(b) for DDP<sub>15</sub>M<sub>5</sub>H<sub>50</sub> model



(c) for DDP<sub>10</sub>M<sub>10</sub>H<sub>50</sub> model



(d) for DDP<sub>15</sub>M<sub>10</sub>H<sub>50</sub> model

Fig. 11 Displacement response when the bearing plate embedded at 0.5 B depth

the variation of depth of bearing plate (0, 0.5B, B, and 2B). The displacement inside the soil medium was obtained by using FFT analysis and processing software (visual log-data analysis software DFA-7610) to get the velocity and displacement from acceleration results.

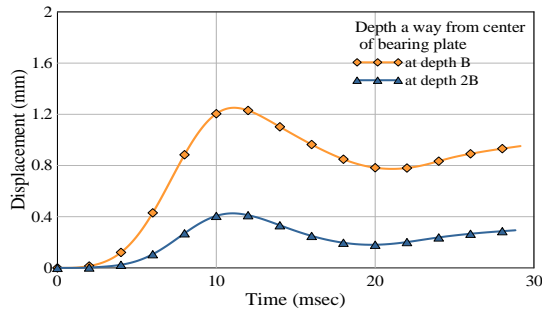
The function of the falling weight deflectometer (FWD) is adopted by dropping freely a mass from a certain height over a plate (used to be at top of soil surface or embedded within the soil) and at the same time recording the impact load-time history developed in the load cell that is attached to the top of the plate. Several notes can be drawn from

Figs. 6 to 13, as illustrated in the following sections.

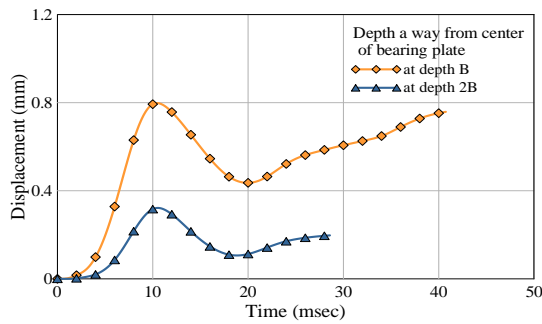
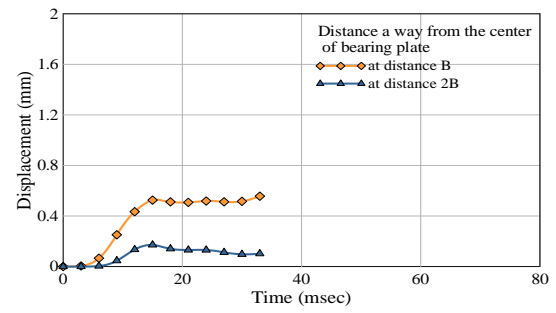
### 3.1 Displacement response

The term displacement response refers to top soil surface displacement under impact force in the vertical direction (measured under the center of the impact plate); these responses are shown at the lower segment of part (a) of Figs. 6 to 9. There are common trends associated with impact, these are:

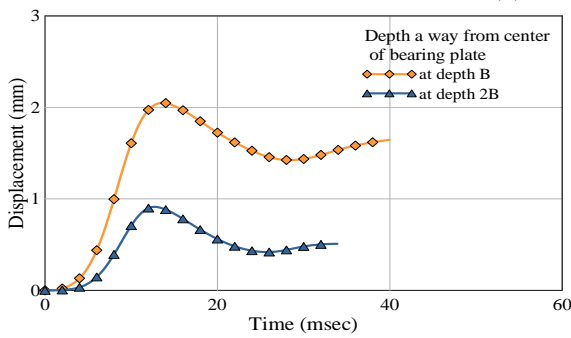
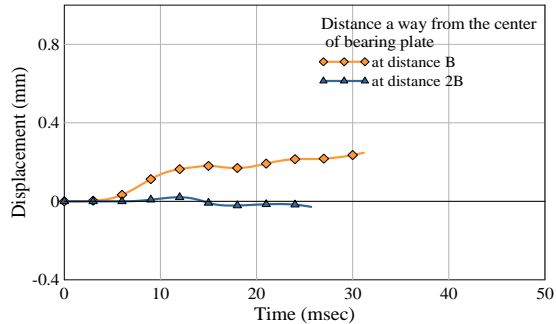
- a. Maximum displacement occurs always when the



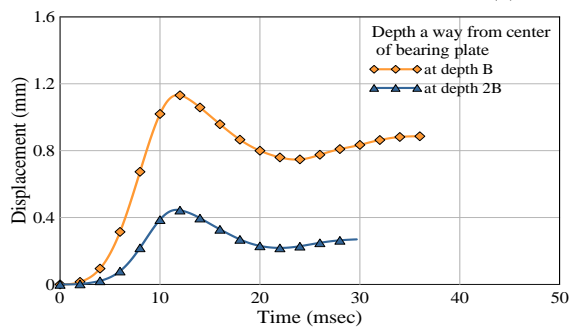
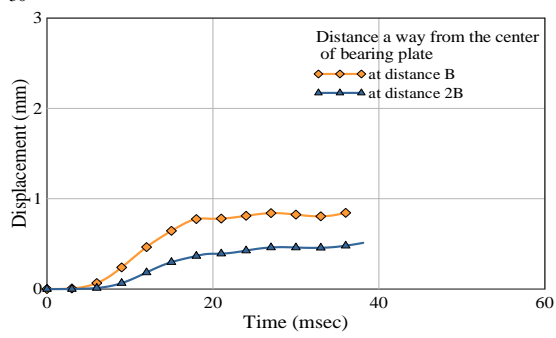
(a) for  $DDP_{10}M_5H_{50}$  model



(b) for  $DDP_{15}M_5H_{50}$  model



(c) for  $DDP_{10}M_{10}H_{50}$  model



(d) for  $DDP_{15}M_{10}H_{50}$  model

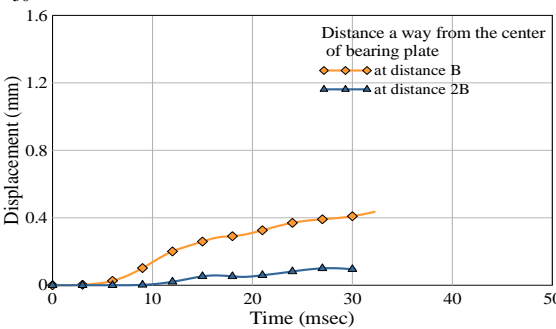


Fig. 12 Displacement response when the bearing plate embedded at B depth

impact plate is located at top soil surface, as the impact plate is embedded at deeper locations, the surface displacement reduces. This is clearly shown in Figs. 10 to 13. This tendency is related to the increase in the compressible layer subjected to impact loads. When the embedment depth increased, this will lead to increasing the overburden pressure which in turn leads to rebound and increasing in the points of contact between particles and more uniform contact pressure which results in increasing in the stiffness of the sandy soil. The reductions in the values of displacement when the plate is embedded at 2B as

compared to the case when the plate is located at top soil surface ranges from 40-45% in most cases. Exception to this trend was obtained when the plate diameter is 100 mm and acted upon by 5 kg falling mass from 250 mm height where the reduction in displacement is about 50% for the two cases of plate depths. The same observation was noticed by Al-Homoud and Al-Maaitah (1996), Mandal and Roychowdhury (2008), Al-Azawi *et al.* (2006), Prakash and Puri (2006), Al-Ameri (2014), Bhandari and Sengupta (2014), and Fattah *et al.* (2015). They attributed this trend to the trench effect (the normal and shear stresses resulting

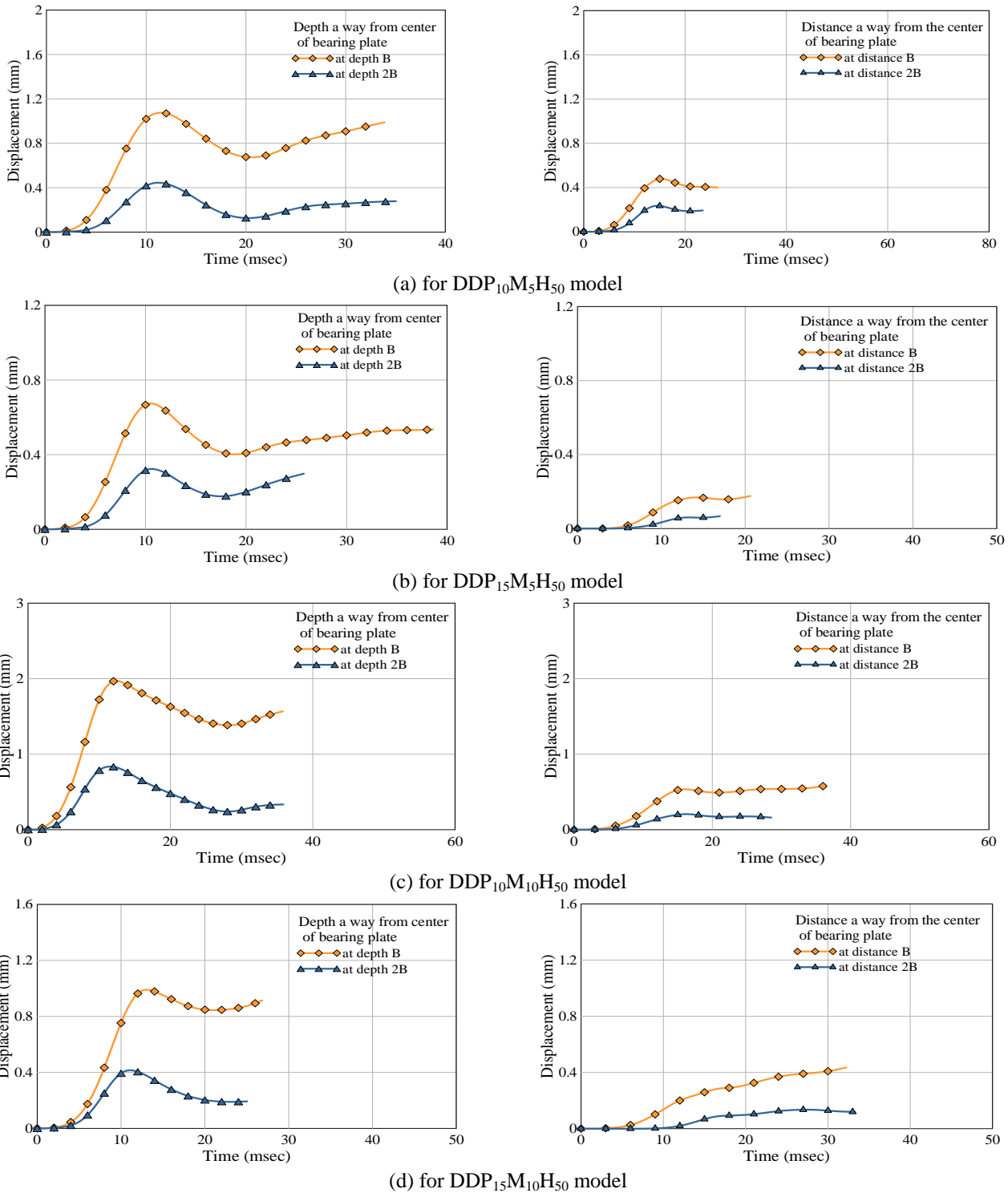


Fig. 13 Displacement response when the bearing plate embedded at 2B depth

from the overlying soil restrict the vertical movement and thus reduce the settlement of the foundation base by increasing its vertical stiffness) and sidewall effects (part of the applied load is transmitted to the ground through shear stresses along the vertical sides of the footing when the sides are in contact with the surrounding soil).

b. At the same energy of impact, the displacement reduces with the increase of footing diameter (hence, footing area). This is clearly shown in Figs. 10 to 13. The

reduction in displacement was found to be ranging from 30% to 40% when the plate is located at the top soil surface. If the plate is embedded at a depth of 2B, the difference becomes in the range from 30% to 35%. It is worth mentioning that the area of impact plate is increased by 125% with the increase of footing diameter. Al-Homoud and Al-Maaitah (1996), Fattah *et al.* (2014), Al-Ameri (2014) found the same trend, that is, when the area of foundation increases, the oscillation of vertical

displacement decreases, which means that the foundation becomes more stable and the reduction in response for large contact area is attributed to the reduction in the stresses due to large contact area.

Al-Homoud and Al-Maaitah (1996) found that there is an increase in natural frequency and reduction in amplitude with the increase in footing base area. The increase in natural frequency is verified in this study.

The special notes that are related to the dynamic behavior of foundation-soil system are:

a. The peak response occurs during the active phase of the pulse (within the phase of forced vibration), this means that the frequency of the applied load ( $\bar{\omega}$ ) is less than the natural frequency of the soil-foundation system ( $\omega$ ) or ( $\beta = \frac{\bar{\omega}}{\omega} < 1$ ).

b. When the impact plate is embedded at a depth of 2B below the top surface of the soil, the peak response occurs within a relatively short duration after the peak impulse occurs (at a time lag of 22% to 35% of the time of peak impulse). The maximum phase angle (time lag) occurs always when the impact plate is located at the top surface of the soil. The time lag is found to be ranging from 40% to 65% of the time of peak impulse. The time of the peak impulse ranges from 8.05 msec to 11.35 msec, and the time of the peak response ranges from 11.25 msec to 17.0 msec. As an example, in case of  $DD_{5P_{10}}M_{10}H_{50}$ , the time of the peak impulse is about 9.85 msec, and the time of the peak response is about 16.2 msec, while in case of  $DD_{2bP_{10}}M_{10}H_{50}$  model the time of the peak impulse is about 10.1 msec and the time of the peak response is about 13.4 msec. This means that, although the peak response is still within the active phase of the impact but however, the frequency ratio ( $\beta$ ) is approaching a value near to 1.0 ( $\bar{\omega}$  approaches  $\omega$ ).

c. It is important to notice from figures in part "b" of each plot that, the pulse wave velocity at the end of the active phase of the impulse is always having low magnitude or sometimes approaching to zero. This means that although the displacement response occurs at the end of the active phase of loading however, the maximum response never occurs during the free vibration phase (after the end of the impulse). Such a tendency proves that the dynamic response vanishes quickly due to large absorption of the energy.

d. The acceleration of the pulse curve is noticed from figures in part "c" to vanish at the end of the pulse interval in most cases as the pulse velocity dose.

The impact force-time curves are almost ideally harmonic in nature; but of a single pulse, with a negative phase. This negative phase might resemble the rebound of the soil-structure to the falling mass; the system in such a case is acting as an elastic body responding to the impact load. In case of medium sand, no such tendency is being observed, the impulse force-time pulse is no longer being a sine pulse, and that is, the soil is acting as a visco-elastic medium. The impact forces do not end to zero but instead end to values equal to the static weight of the falling mass or less, that is, no rebound.

The maximum displacement occurs always when the impact plate is located at the top soil surface, as the impact plate is embedded at deeper locations, the surface

displacement reduces, and the reduction in the displacement occurs due to the decrease in pressure when the area of the plate increases.

#### 4. Conclusions

1. The maximum displacement occurs always when the impact plate is located at top soil surface, as the impact plate is embedded at deeper locations, the surface displacement reduces. The reductions in the values of displacement when the plate is embedded at 2B as compared to the case when the plate is located at top soil surface ranges from 40-45% in most cases
  2. The peak displacement response was found to take place during the active phase of the pulse (within the phase of forced vibration), this means that the frequency of the applied load ( $\bar{\omega}$ ) is less than the natural frequency of the soil-foundation system ( $\omega$ ) or ( $\beta = \frac{\bar{\omega}}{\omega} < 1$ ).
  3. The embedment depth of the foundation has a considerable effect. When the impact plate is embedded at a depth of 2B below the top surface of the soil, the peak response occurs within a relatively short duration after the peak impulse occurrence (at a time lag of 22% to 35% of the time of peak impulse). The maximum phase angle (time lag) occurs always when the impact plate is located at the top surface of the soil. The time lag is found to be ranging from 40% to 65% of the time of peak impulse.
  4. The frequency ratio (frequency of the impact/frequency of the vibration foundation-soil system) is very important factor in problems deal with impact load.
  5. The amplitude of the force-time history for dense soil under impact load is ideally harmonic with a single pulse.
  6. Increasing the footing embedment depth results in the following conclusions:
    - a. Amplitude of the force-time history increases by about 10-30% due to increase in the degree of confinement.
    - b. The displacement response of the soil will decrease by about 40-50% for dense sand due to increase in the overburden pressure which leads to increase in the stiffness of the sandy soil.
    - c. Increasing the natural frequency of the soil-foundation system ( $\omega$ ) by about 20-45%. For surface foundation, the foundation is free to oscillate in vertical, horizontal and rocking modes. But, when embedding a footing, the surrounding soil restricts oscillation due to confinement which leads to increasing the natural frequency. Moreover, the soil density increases with depth because of compaction.
    - d. Increase in the value of total active mass for dense soil by about 10-25% hence, increasing amplitude of the fore-time history and creating more wave travel paths.
    - e. An increase in the modulus of subgrade reaction, modulus of elasticity, and shear modulus by about 50-100% due to the increase in soil density.
- An increase in the damping ratio by about 50-150% due to the increase of soil density as D/B increases, hence the

soil tends to behave as a solid medium which activates both viscous and strain damping.

## References

- Al-Ameri, A.F.I. (2014), "Transient and steady state response analysis of soil foundation system acted upon by vibration", Ph.D. Thesis, Civil Engineering Department, University of Baghdad, Iraq.
- Al-Azawi, T.K., Al-Azawi, R.K. and Al-Jaberi, Z.K. (2006), "Stiffness and damping properties of embedded machine foundations", *J. Eng., Univ. Baghdad*, **12**(2), 429-443.
- Al-Homoud, A.S. and Al-Maaitah, O.N. (1996), "An experimental investigation of vertical vibration of model footings on sand", *Soil Dyn. Earthq. Eng.*, **15**(7), 431-445.
- Al-Saffar, F.S.M. (2015), "Dynamic behavior of machine foundation resting on piles in a sandy soil", Ph.D. Thesis, Civil Engineering Department, University of Baghdad, Iraq.
- American Society of Testing and Materials (ASTM) (1969), Standard Test Method for Relative Density of Cohesionless Soils, ASTM D 2049-69 International, West Conshohocken, Pennsylvania, USA.
- American Society of Testing and Materials (ASTM) (2000), Standard Test Method for Minimum Index Density and Unit Weight of Soils and Calculation of Relative Density, ASTM D4254-00 International, West Conshohocken, Pennsylvania, USA.
- American Society of Testing and Materials (ASTM) (2006), Standard Test Method for Particle Size-Analysis of Soils, ASTM D422-02, West Conshohocken, Pennsylvania, USA.
- American Society of Testing and Materials (ASTM) (2006), Standard Test Method for Specific Gravity of Soil Solids by Water Pycnometer, ASTM D854, West Conshohocken, Pennsylvania, USA.
- Bhandari, P.K. and Sengupta, A. (2014), "Dynamic analysis of machine foundation", *Int. J. Innov. Res. Sci. Eng. Technol.*, **3-4**, 169-176.
- Das, B.M. and Ramana, G. (2011), *Principles of Soil Dynamics*, CI-Engineering.
- Davies, M.C.R., Bowman, E.T. and White, D.J. (2010), "Physical modelling of natural hazards", *Physical Modelling in Geotechnics, Two Volume Set: Proceedings of the 7th International Conference on Physical Modelling in Geotechnics (ICPMG 2010)*, June-July, Zurich, Switzerland
- Fattah, M.Y., Al-Mosawi, M.J. and Al-Ameri, A.F.I. (2017), "Stresses and pore water pressure induced by machine foundation on saturated sand", *Ocean Eng.*, **146**, 268-281.
- Fattah, M.Y., Hamood, M.J. and Abbas, S.A. (2014), "Behavior of plate on elastic foundation under impact load", *Eng. Technol. J.*, **32**(4), 1007-1027.
- Fattah, M.Y., Salim, N.M. and Al-Shammmary, W.T. (2015), "Effect of embedment depth on response of machine foundation on saturated sand", *Arab. J. Sci. Eng.*, **40**(11), 3075-3098.
- Guellil, M.E., Harichane, Z., Djilali Berkane, H. and Sadouki, A. (2017), "Soil and structure uncertainty effects on the soil foundation structure dynamic response", *Earthq. Struct.*, **12**(2), 153-163.
- Jayalekshmi, B.R., Thomas, A. and Shivashankar, R. (2014), "Dynamic soil-structure interaction studies on 275 m tall industrial chimney with openings", *Earthq. Struct.*, **7**(2), 233-250.
- Kumar, S.S., Krishna, A.M. and Dey, A. (2013), "Parameters influencing dynamic soil properties: A review treatise", *National Conference on Recent Advances in Civil Engineering*, November.
- LS-DYNA Keyword User's Manual (2009), Volume 1, Livermore Software Technology Corporation (LSTC).
- Mandal, J.J. and Roychowdhury, S. (2008), "Response of rectangular raft foundations under transient loading", *Proceedings of the 12th International Conference of International Association for Computer Methods and Advanced in Geomechanics (IACMAG)*, India.
- Plaxis 2D General Manual (2017), Delft University of Technology and Plaxis bv, the Netherlands.
- Prakash, S. and Puri, K.V. (2006), "Foundation for vibrating machines", *J. Struct. Eng.*, **33**(1), 13-29.
- ProShake Ground Response Analysis Program Version 2.0 User's Manual, EduPro Civil Systems, Inc. Sammamish, Washington.
- Svinkin, M.R. (2008), "Soil and structure vibrations from construction and industrial sources", *Proceedings of the Sixth International Conference on Case Histories in Geotechnical Engineering*, Omni Press, Arlington, Virginia.
- Turner, J.R. and Kulhawy, F.H. (1987), "Experimental analysis of drilled foundations subjected to repeated axial loads under drained conditions", Report EL-S32S, Electric Power Research Institute, Palo Alto, California.
- Xue, X., Ren, T. and Zhang, W. (2012), "Analysis of fatigue damage character of soils under impact load", *J. Vib. Control*, **19**(11), 1728-1737.

CC